

Epigenetic Lead, Zinc, Silver, Antimony, Tin and Gold Veins in Boulder Basin, Blaine and Custer Counties, Idaho— Potential for Economic Tin Mineralization

By Michael E. Ratchford

U.S. Geological Survey Bulletin 2064-JJ

*Prepared in cooperation with the Idaho Geological Survey,
Idaho State University, and the University of Idaho*

U.S. Department of the Interior
U.S. Geological Survey

U.S. Department of the Interior
Gale A. Norton, Secretary

U.S. Geological Survey
Charles G. Groat, Director

This publication is only available online at:
<http://geology.cr.usgs.gov/pub/bulletins/b2064-jj/>

Version 1.0 2002

Any use of trade, product, or firm names in this publication
is for descriptive purposes only and
does not imply endorsement by the U.S. Government

Published in the Central Region, Denver, Colorado
Manuscript approved for publication June 27, 2002
Graphics by Dave Walters and Gayle M. Dumonceaux
Photocomposition by Gayle M. Dumonceaux

Contents

Abstract	1
Introduction	1
Geologic Setting	3
Host Rocks	3
Host Structures	4
Mineral Deposits	6
Ore Geochemistry.....	8
Ore Microscopy and Electron Microprobe Results.....	9
Geophysical Signature	13
Genesis and Ore Controls	14
Potential for Economic Tin Mineralization	14
Exploration Guides	14
References	15

Figures

1. Simplified geologic map of the black shale mineral belt of central Idaho	2
2. Photograph of the Boulder Basin cirque.....	3
3. Schematic diagram illustrating the stages of development for the Boulder Basin thrust fault and overlying roof thrust fault.....	4
4. Schematic diagram illustrating the relation between the kinematic movement indicators to the roof thrust fault and the spatial relation to the underlying Boulder Basin thrust fault	5
5. Oriented thin section from the roof thrust fault.....	6
6. Schematic diagram of structural features of Boulder Basin.....	7
7. Photograph of the mine town in Boulder Basin.....	8
8. Graphs showing concentrations of silver, copper, and antimony versus tin in ore samples from Boulder Basin.....	9
9. Photomicrograph of mineralized sample from Boulder Basin.....	13

Tables

1. Geochemical analyses of ore specimens from Boulder Basin.....	10
2. Microprobe analyses of galena from Boulder Basin	12

Metric Conversion Factors

Multiply	By	To obtain
Miles	1.609	Kilometers
Feet	0.3048	Meters
Inches	2.54	Centimeters
Tons	1.016	Metric tons
Short tons	0.907	Metric tons
Troy ounces	31.103	Grams
Ounces	28.35	Grams

Epigenetic Lead-Zinc-Silver-Antimony-Tin and Gold Veins in Boulder Basin, Blaine and Custer Counties, Idaho—Potential For Economic Tin Mineralization

By Michael E. Ratchford

Abstract

Boulder Basin is in a northwest-trending belt of allochthonous Paleozoic rocks in the Boulder Mountains of central Idaho. Regional Tertiary extension resulted in widespread normal faulting and coeval emplacement of shallow-level intrusions and extrusive rocks of the Challis Volcanic Group. Epigenetic lead-zinc-silver-antimony-tin-gold vein deposits formed during Tertiary extension and are hosted within Paleozoic strata. The major orebodies are in the lower plate of the Boulder Basin thrust fault, in massive quartzite of the Middle Pennsylvanian to Lower Permian Wood River Formation. Anomalous concentrations of tin are present in the base-metal mineral assemblage of the Boulder Basin ore deposits. The tin-bearing veins in Boulder Basin are strikingly similar to Bolivian tin deposits. The deposit model for Bolivian tin deposits identifies buried tin porphyry below the tin-bearing vein system.

Introduction

Boulder Basin is 22 km northwest of Ketchum, Idaho (fig. 1), in the southern Boulder Mountains. The geology of Boulder Basin consists of a Tertiary hypabyssal-volcanic complex that intruded metasedimentary and sedimentary rocks of the Devonian Milligen Formation and Middle Pennsylvanian to Lower Permian Wood River Formation. Numerous dikes, sills, and small intrusions of andesite, dacite, and rhyolite porphyry constitute approximately 50 percent of the surface exposures. In places, feeder dikes of these rocks merge upward into overlying lavas of the Challis Volcanic Group, whereas in other areas these intrusive rocks crosscut the volcanic stratigraphy. Epigenetic lead-zinc-silver-antimony-tin-gold vein ore deposits formed during Tertiary extension and are similar to Bolivian tin deposits (Taylor, 1979, p. 492–493). The primary objectives of this study were to determine the stratigraphic and structural controls of mineralization and the potential for economic tin mineralization. The data and conclusions presented in this paper are based, for the most part, on Ratchford (1989).

Both patented and unpatented mining claims are present in and adjacent to Boulder Basin. Most of the ore produced from the area is from patented claims which were originally held by

two companies, the Golden Glow Mining Co. and the Boulder Consolidated Mining Co. The Golden Glow group of claims, patented between 1883 and 1892, consisted of the Lousia, Ohio, Sunrise, Ophir, and Bazouk claims (Van Noy and others, 1986, p. 421–436). The Boulder Consolidated group of claims bordered the Golden Glow group and included the Triumph, Sunset, Summit, Crown Point, Calamine, Daisy, Puritan, Champion, Climax, Revenue, Mascot, and Mint claims, which were patented in 1929 (Van Noy and others, 1986, p. 421–436). Currently, both the patented and unpatented claims in the area are inactive, and have had only intermittent activity between 1890 and 1949.

In the first account of Boulder Basin mines, Umpleby (1915) concluded that most production was prior to 1890 and principally from the original Golden Glow group of claims. Although no production records exist prior to 1902, Umpleby (1915) estimated that \$1,000,000 worth of ore was shipped prior to 1890; he gave no explanation as to how he derived the estimate. However, the price of gold at the time he published the \$1,000,000 estimate was \$20.67/troy ounce suggesting 48,379 ounces extracted gold.

In the mid-1970's, the U.S. Geological Survey and the U.S. Bureau of Mines conducted surface and subsurface geologic mapping and sampling of Boulder Basin mines as part of a mineral resource assessment of the Sawtooth National Recreation Area (Van Noy and others, 1986; Tschanz and Kiilsgaard, 1986). During this study, it was concluded that base metal veins that had been mined for silver, lead, and zinc also contained quantities of tin, which previously had not been recognized. The tin-bearing veins were in an arcuate belt that extends from Boulder Basin in the south to the Salmon River drainage in the north (Van Noy and others, 1986, p. 145–152). The Galena and Fourth of July Creek districts were delineated as areas that contained appreciably higher tin concentrations than the rest of the belt. A complex ore mineral assemblage of silver sulfosalts, cassiterite (SnO_2), tellurian canfieldite ($\text{Ag}_8\text{Sn}(\text{Se}, \text{Te})_6$), and several members of the sulfidic stannite family ($\text{Cu}_2\text{FeSnS}_4$) was identified in these two districts (Van Noy and others, 1986, p. 97–98, p. 145–152).

Paul (1981) studied the ore mineral assemblage in the Galena district and identified 13 ore minerals, including the tin-bearing phases: stannite ($\text{Cu}_2\text{FeSnS}_4$), cassiterite (SnO_2), and varlomoffite ($\text{Sn,Fe}(\text{O},\text{OH})_2$). Stannite was reported to be the most abundant tin ore mineral.

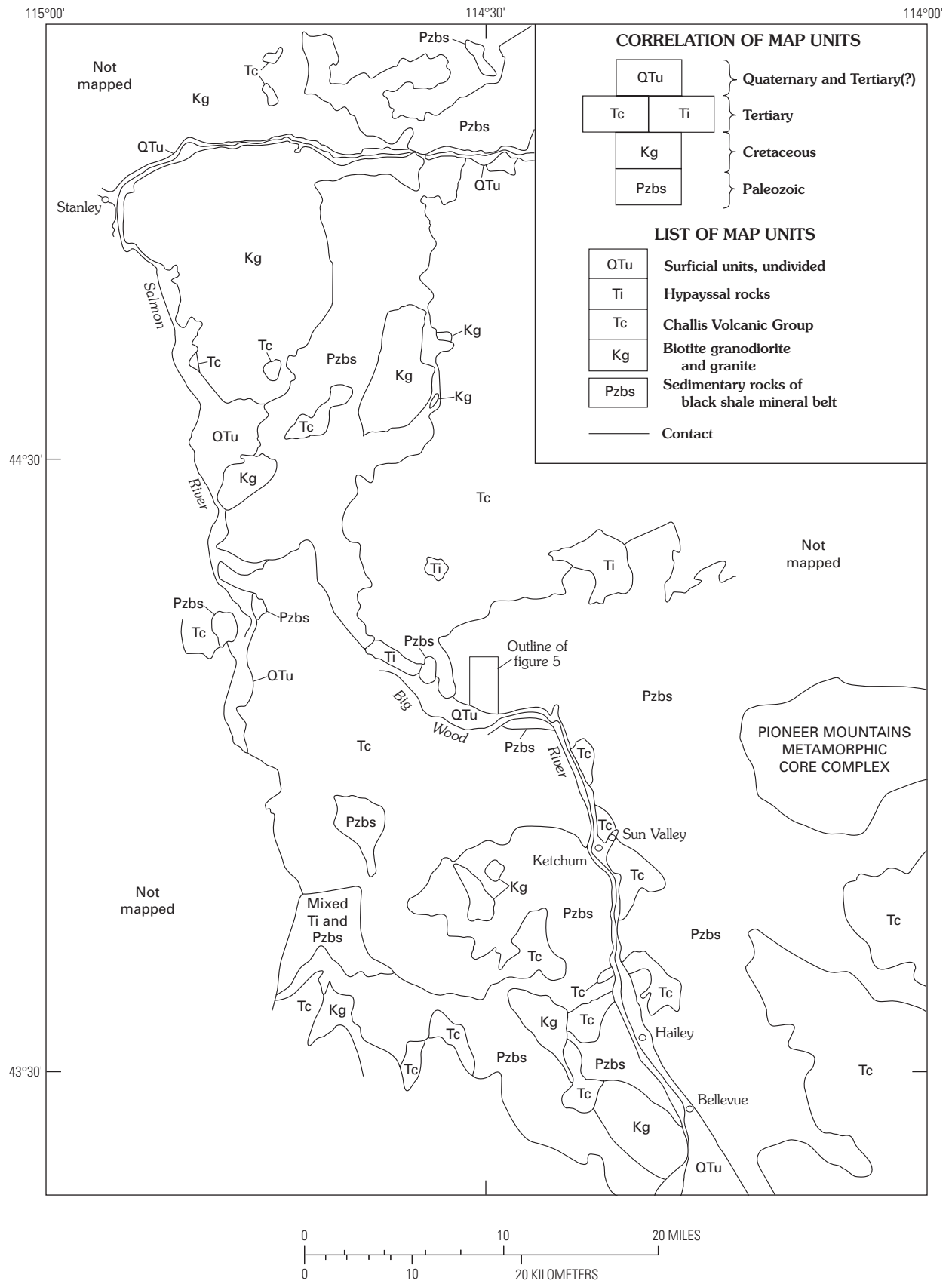


Figure 1. Simplified geologic map of the black shale mineral belt of central Idaho. Modified from Hall (1985).



Figure 2. Photograph of the Boulder Basin cirque, central Idaho. The main ore bodies are in the right-central part of the photograph. The tallest peak in the background, Boulder Peak, has an elevation of 10,981 ft.

Geologic Setting

Boulder Basin is in a northwest-trending belt of allochthonous lower Paleozoic carbonaceous sedimentary rocks and upper Paleozoic siliclastic and calcareous rocks. This assemblage of rocks was named the central Idaho black shale belt by Hall (1985) and extends from approximately 8 km south of Bellevue, Idaho to just north of the Salmon River (fig. 1). The western margin of this belt is adjacent to the Atlanta lobe of the Idaho batholith and the eastern margin flanks the west side of the Boulder and Pioneer Mountains. Several Cretaceous stocks that are outliers of the Idaho batholith intrude the Paleozoic sedimentary units along the western margin of the black shale belt. Regional Tertiary extension resulted in widespread normal faulting and coeval eruption of the Challis volcanic sequence and emplacement of hypabyssal intrusions into Paleozoic strata.

The Devonian Milligen Formation and the Pennsylvanian to Permian Wood River Formation make up the greatest areal extent of sedimentary rocks in the black shale belt. Field relations suggest that the Wood River Formation was deposited unconformably on the Milligen Formation and that both formations were folded and thrust during the Sevier orogeny. Regional extension that overprints the compressional fabric of the Paleozoic strata included widespread normal faulting and reactivation of earlier compressional structures.

Hall and others (1978) and Hall (1985) defined the Milligen-Wood River contact as the regional Wood River thrust

fault. Field research in the present study locally confirmed Hall's interpretation of the nature of this contact; however, in places the Milligen-Wood River contact was also mapped as a sheared unconformity with isolated remnant slices of depositional continuity, as a normal fault, and as a reactivated thrust fault with a normal sense of movement (Ratchford and Reid, 1993).

Host Rocks

Both the Milligen and Wood River Formations are host rocks for ore deposits in and adjacent to Boulder Basin. The Milligen stratigraphic section is incomplete in the study area due to erosion, faulting, assimilation by Tertiary intrusions, and lack of exposures. The structural and stratigraphic relations of the Milligen Formation are poorly understood, due to a complicated deformational history, repetition of similar lithologies throughout the Milligen stratigraphy, and limited age constraints. The stratigraphy of the Milligen Formation was reviewed by Turner and Otto (1988) and Sandberg and others (1975). The lithostratigraphy proposed by Turner and Otto (1988) has no fossil control and the biostratigraphy of Sandberg and others (1975) has sparse fossil control in two incomplete stratigraphic sections.

Sandberg and others (1975) divided the Milligen Formation into a carbonaceous and phyllitic lower member and a more siliceous and heterogenous upper member. Most of the

Milligen Formation in Boulder Basin is near the top of the stratigraphic section, on the basis of lithostratigraphic comparisons of similar stratigraphic intervals throughout the Milligen terrane. The uppermost part of the Milligen lithostratigraphy defined by Turner and Otto (1988) is principally green shale, which is correlated with the Milligen strata in Boulder Basin.

The Milligen stratigraphic section in Boulder Basin is primarily dark-green, fissile shale that is interbedded with lesser black chert, gray sandy limestone, gray calcareous quartzite, and black phyllite. The green shale is the primary host rock for mineralization in Milligen strata. The only fossils from the Milligen Formation were collected in Boulder Basin from one limestone sample. The sample yielded conodont fragments that were examined by Rachel Paul, University of Wisconsin-Milwaukee, who concluded that the sample was early Late Devonian (Frasmoam) in age (Rachel Paul, Univ. Wis., written commun., 1989).

The stratigraphic section of the Wood River Formation is also incomplete in the Boulder Basin area. It is represented by a relatively thick section of Unit 6 and a small fault sliver of Unit 1 and Unit 2 (unit designations from Hall and others, 1974). Unit 1 is matrix-supported, multilithic, chert-pebble conglomerate. Unit 2 is conformable with Unit 1 and is blue-gray, highly fossiliferous limestone that contains diagnostic rugose corals as large as 10 cm. The principal lithologies in Unit 6 are an alternating succession of brown- to maroon-weathering, fine- to medium-grained, calcareous sandstone and siltite interbedded with light- to dark-gray sandy limestone and fine-grained, siliceous and calcareous gray quartzite. Gray massive quartzite of Unit 6 is the primary host rock for Wood River Formation mineralization in Boulder Basin.

Units 3, 4, 5, and 7 and parts of Units 1, 2, and 6 of the Wood River Formation were not identified in this study because of erosion, faulting, stratigraphic thinning, and intrusive assimilation, as well as lack of exposure.

Host Structures

The major structural feature in Boulder Basin is the Boulder Basin thrust fault, which places the Milligen Formation in the upper plate above the Wood River Formation (Ratchford, 1989, pl. 1, 2). A schematic representation of the development of the Boulder Basin thrust fault is shown in figure 3. The Boulder Basin thrust fault may have initiated in the lower plate of the Wood River thrust fault after the plate became inactive. This interpretation allows the Boulder Basin thrust fault to cut upsection, placing a thickened wedge of the Milligen and Wood River Formations on the Wood River thrust fault in the vicinity of the study area.

A roof thrust fault that structurally overlies the Boulder Basin thrust fault is also shown schematically in figures 3 and 4. Mesoscopic and microscopic kinematic movement indicators in the roof thrust fault indicate eastward direction of tectonic transport. A southeast-verging drag fold is present in the fault, and the orientation of the fold axis is 20°, 215° azimuth. The corresponding slip-line direction of 125° azimuth is perpendicular to the trend of the drag-fold axis.

Oriented samples were collected from the roof thrust fault and cut parallel with stretching mineral lineation. Thus, thin

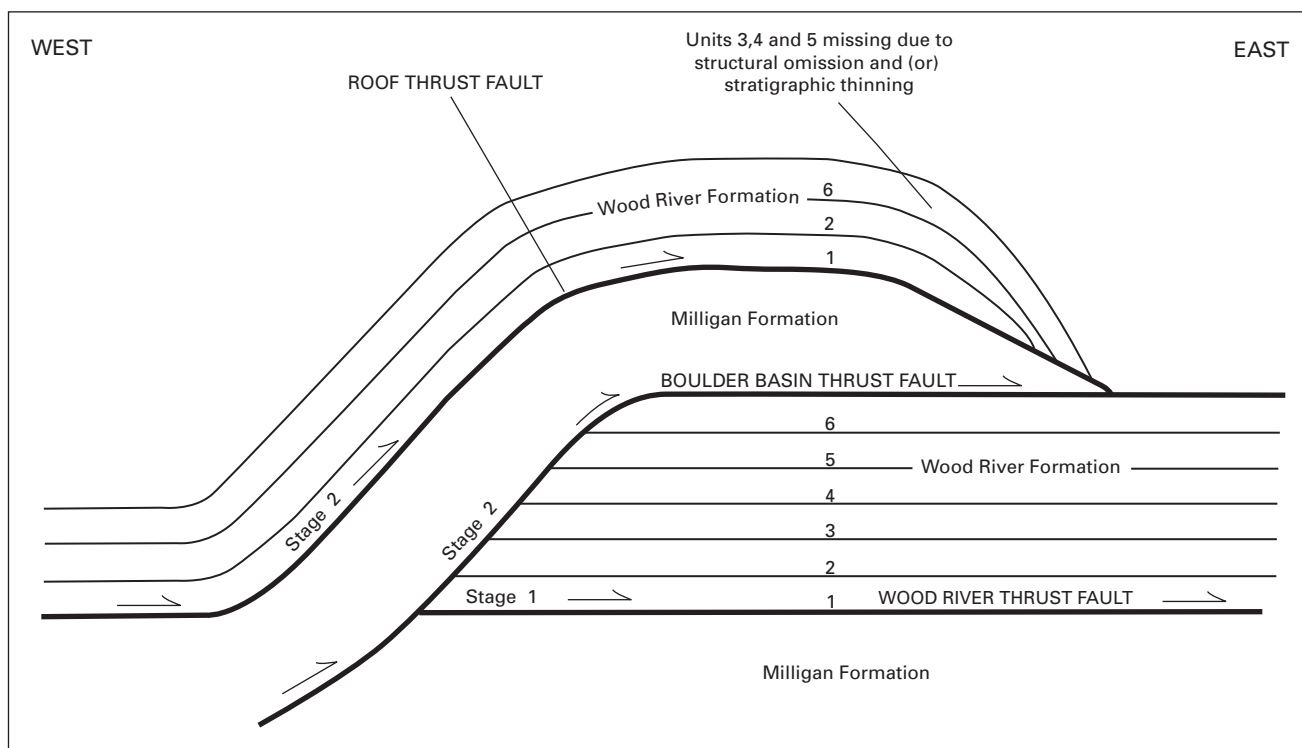


Figure 3. Schematic diagram illustrating the stages of development for the Boulder Basin thrust fault and the overlying roof thrust fault.

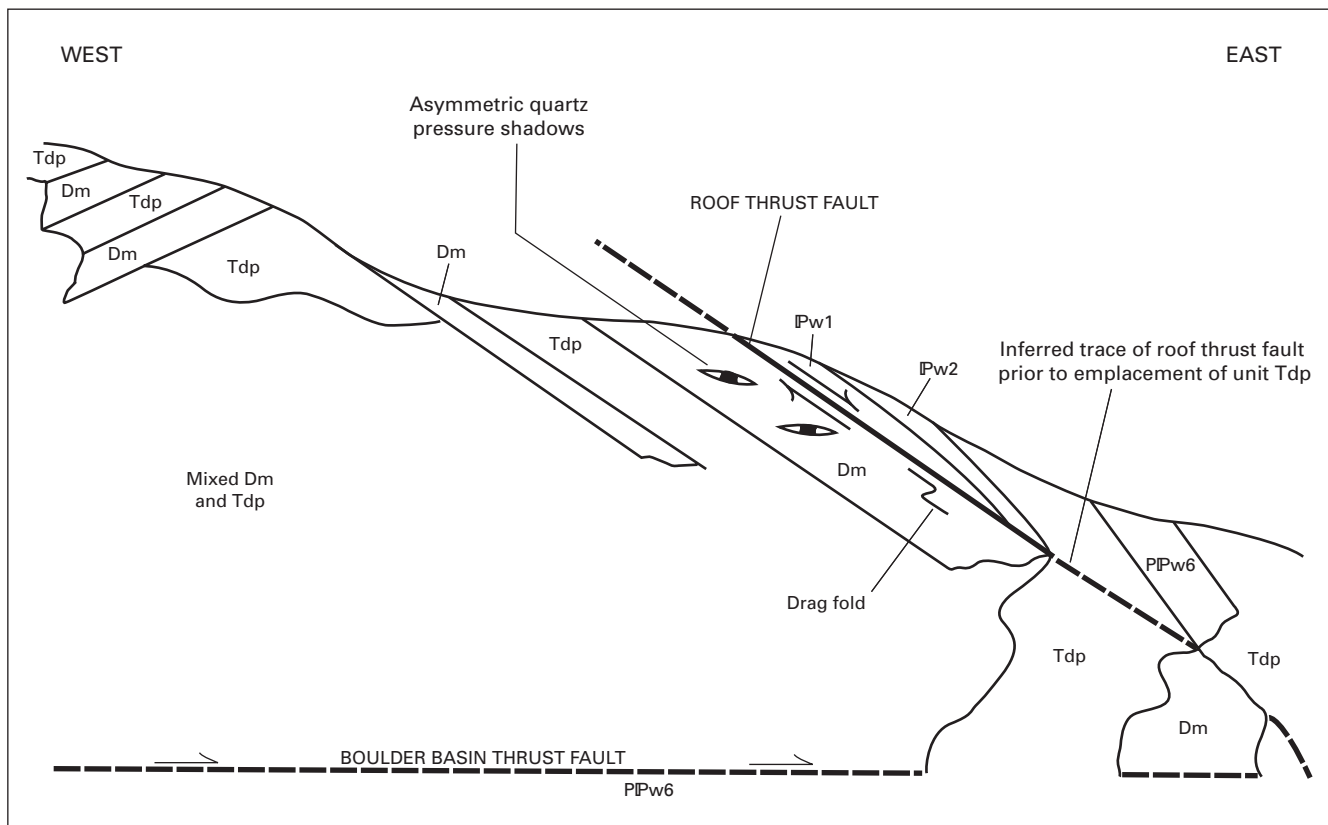


Figure 4. Schematic diagram illustrating the relation between the kinematic movement indicators and the roof thrust fault and the spatial relation to the underlying Boulder Basin thrust fault. Dm, Milligen Formation; IPw1, Unit 1, Hailey Member, Wood River Formation; IPw2, Unit 2, Hailey Member, Wood River Formation; IPPw6, Unit 6, Wood River Formation; Tdp, Tertiary dacite porphyry. Not drawn to scale.

sections from the faces of the oriented samples correspond to the XZ plane of the strain ellipsoid. The thin sections contain asymmetric quartz pressure shadows that are attached to rigid pyrite crystals. Quartz pressure shadows are symmetrically disposed regions of low strain that develop on opposite sides of rigid crystals where the rock matrix is protected from the full effects of deformation (Ramsay and Huber, 1983, p. 265). In the pressure shadow region, the matrix has separated from the rigid pyrite and forms extension fractures that are filled with fibrous quartz. The rigid pyrite crystals were rotated in a ductile matrix of clay and mica, probably by simple shear mechanisms during thrusting. This rotation resulted in one side of the pressure shadow stepping up in the direction of shear, as shown in figure 5. The morphology of the pressure shadows is analogous to sigma- and delta-type porphyroclasts in the classification scheme of Simpson (1986).

Although no reliable kinematic movement indicators were detected from the Boulder Basin thrust fault, an eastward direction of tectonic transport is inferred on the basis of the movement sense and geometry of the overlying roof thrust fault. Visible signs of mineralization are sparse in the upper plate of the Boulder Basin thrust fault; the lower plate hosts the principal mine workings in the study area.

Regional Tertiary extension resulted in development of high- and low-angle faults and brittle shear zones, which overprint the older compressional structures. Although unequivocal kinematic data could not be discerned from the Tertiary faults, a

normal sense of movement is inferred because regional extension was operative during their development.

Mineralized areas in the main mine workings are confined to northeast-trending, southeast-dipping, high-angle, normal(?) faults and brittle shear zones that cut massive quartzite of the Wood River Formation. These structures also cut andesite and dacite porphyry, whereas rhyolite porphyry crosscuts or intrudes the fault and shear planes. All three types of porphyry are identical in appearance to shallow Eocene intrusive rocks throughout the Wood River and Stanley basins that are coeval with the Challis Volcanic Group (Armstrong, 1975, p. 26). On the basis of crosscutting relations of the faults and the porphyries, the faulting and mineralization in the main mine workings probably were restricted to the Eocene. The spatial relation between the mineralized structures and the Boulder Basin thrust fault is shown schematically in figure 6.

Intrusion of rhyolite porphyry, or perhaps deeper level pink granite (potassium feldspar granite), probably provided the heat required to form these hydrothermal ore deposits. This interpretation is based on an observation that mineralized structures postdate andesite and dacite porphyries, whereas rhyolite porphyry clearly was emplaced after the faulting episode that was responsible for hosting of the epigenetic ore deposits. Furthermore, rhyolite porphyry can locally be traced downward into pink granite intrusions throughout the Wood River and Stanley basins (Johnson and others, 1988, p. 60; Bennett and Knowles, 1985, p. 84). Those observations suggest that a pink granite

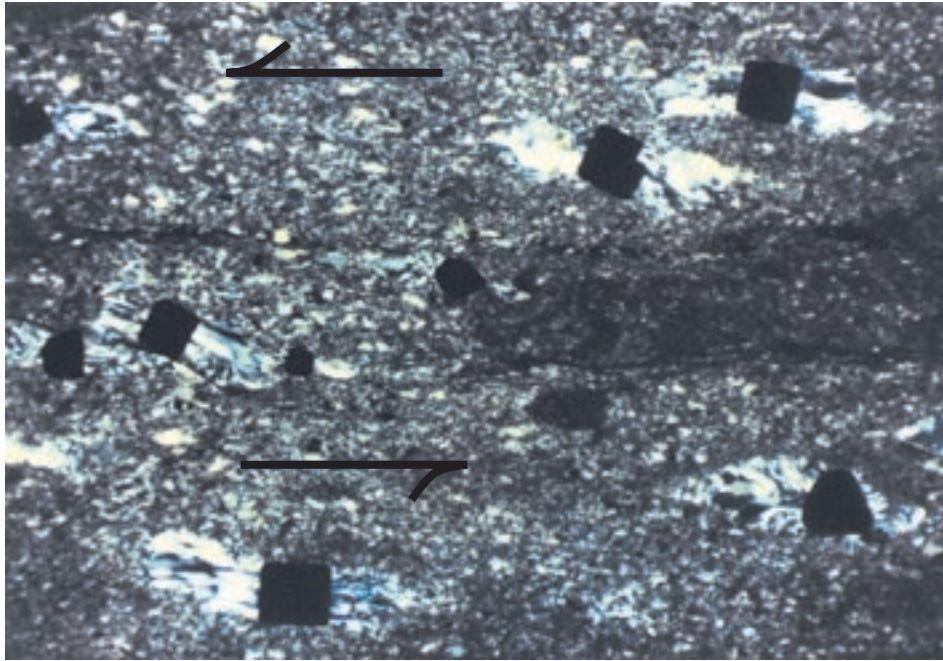


Figure 5. Oriented thin section from the roof thrust plate showing rotated pyrite crystals with asymmetric quartz pressure shadows. Arrows indicate the sense of shear, which corresponds to an eastward direction of tectonic transport. Field of view 8.5 mm.

intrusion is likely present below the main mine workings at Boulder Basin.

Mineralized structures in the principal mine workings range in width from 2.5 cm to approximately 2 m; most average about 26 cm wide. These structures can be easily identified on surface exposures because they are marked by conspicuous hematite and limonite alteration along fault traces. Most of the adits that are open at Boulder Basin mines are driven along the faults and brittle shear zones. Underground mine workings reveal much longer strike lengths to mineralized structures than are exposed on the surface.

A low-angle ($5\text{--}20^\circ$) mineralized Tertiary fault that is not associated with the principal mine workings is in the northwest corner of the cirque headwall in Boulder Basin, below Peak 10,850. An adit driven into this structure exposes stringers of galena and sphalerite in fault gouge of drusy quartz. This fault cuts andesite volcanic flows of the Challis volcanic sequence and Eocene andesite, dacite, and rhyolite porphyry, as well as limestone and quartzite of Unit 6 of the Wood River Formation. Because this fault cuts rhyolite porphyry, and is unusually low-angle for a Tertiary structure in Boulder Basin, it may have been a conduit for fluids during a later mineralizing event. Such low-angle normal faults are known to locally displace older, high-angle Tertiary structures in the Wood River Basin, as discussed by Turner and Otto (1988, p. 164) and as shown by Worl and others (1991). The observations and hypotheses mentioned above may be important to future exploration of Tertiary mineralized rock in the Wood River and Stanley Basins.

Other mineralized Tertiary faults are south of Boulder Basin, on the steep canyon walls east and west of Boulder Creek. The degree of contact metamorphism in the Wood River Formation is generally higher in this area than the degree of contact

metamorphism in similar strata in the main mine workings, probably because it was closer to the roots of the hypabyssal complex. The metaquartzites of the Wood River Formation are highly bleached with purple, green, and red bands. Stringers and veinlets of galena, sphalerite, and pyrite with malachite and azurite staining are exposed in brittle faults and shear zones that cut the metaquartzite. The latter structures generally have a strike length of less than 10 m and are typically 25 cm or less in width. These structures have an average trend of $35^\circ\text{--}60^\circ$ azimuth, and they dip steeply to the northwest and southeast. Faulting and mineralization probably were coeval with formation of the main orebodies in Boulder Basin, as indicated by the cross-cutting relations of faults and intrusive rocks. Van Noy and others (1986, p. 433–436) discussed many of the mineral deposits within this area including the Snug prospect, the Utah group, and the Crown Point and Puritan claims. Field observations in this area indicate that these deposits are of very low tonnage and that mineralized structures commonly pinch out abruptly where roof pendants terminate at intrusive contacts. The primary constraints for the economic viability of these deposits probably are the small size of the mineralized roof pendants and the large volume of barren intrusive rock.

Mineral Deposits

The Boulder Basin and adjacent study area is approximately 10 km southeast of the Galena district. The type and age of mineralization and the host rock for the ore deposits in Boulder Basin are likely the same as those in the Galena district. On the basis of these similarities and the close proximity of the two

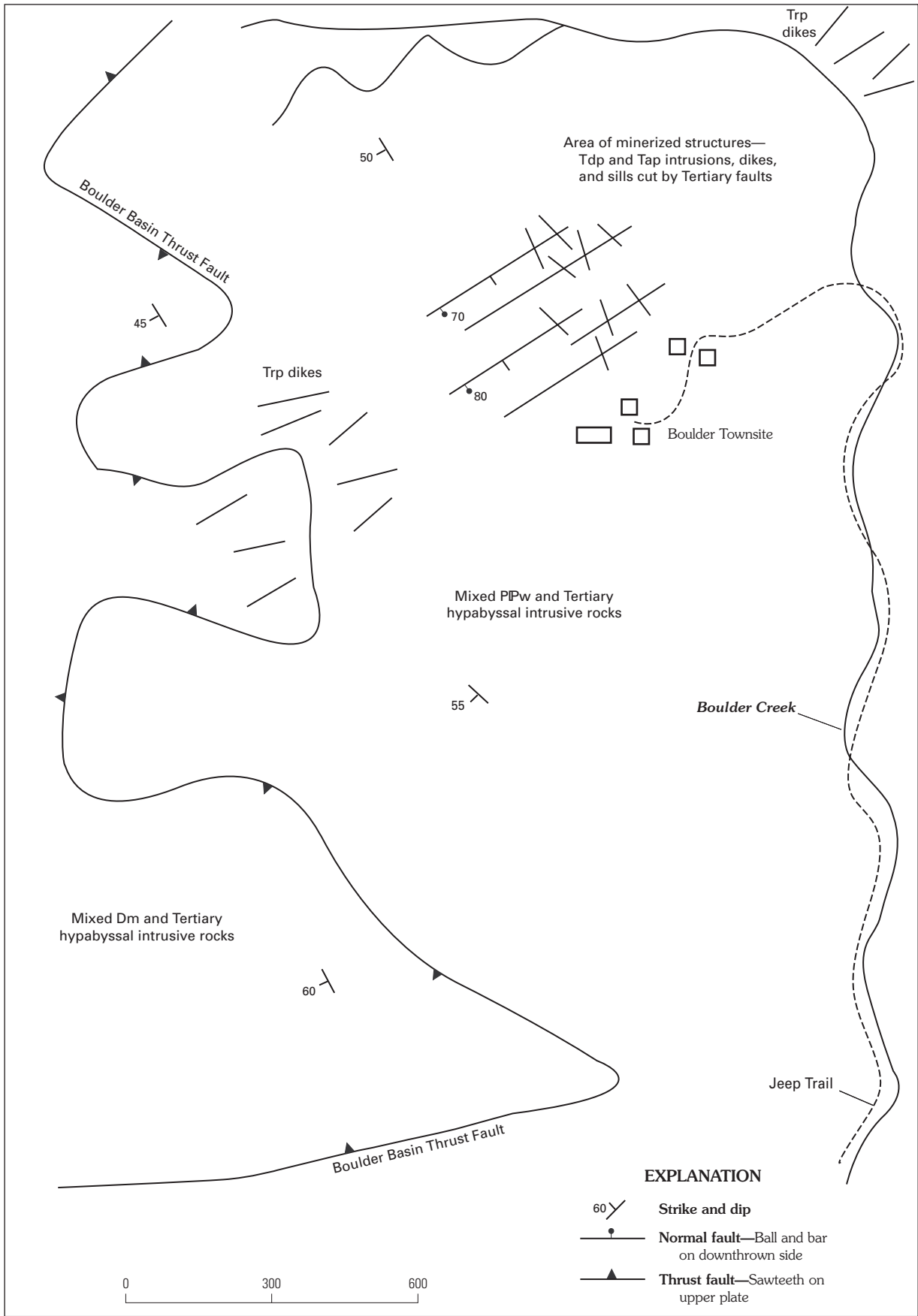


Figure 6. Schematic diagram of the structural features in Boulder Basin. Stratigraphic units: Dm, Milligen Formation; PPw, Wood River Formation; Tap, Tertiary andesite porphyry; Tdp, Tertiary dacite porphyry; Trp, Tertiary rhyolite porphyry.

mining districts, ore deposits in Boulder Basin may have some potential for tin mineralization.

Numerous adits, shafts, and prospects are in and adjacent to Boulder Basin. The principal mine workings are adjacent to an abandoned mine town that is referred to as the Boulder Site on the Easley Hot Springs 7 1/2-minute quadrangle. The remains of a mill, several cabins, ore bins, and tram cables are still present (fig. 7).

The ore deposits in Boulder Basin are hydrothermal, epigenetic lead-zinc-silver-antimony-tin-gold veins that were emplaced by open-space and fissure-filling mechanisms. Sulfide ore is exposed discontinuously along the strike of the mineralized structures as lenses and stringers in fault gouge and breccia; minor to negligible disseminations of sulfide minerals are present in the adjacent wallrock. Hand samples of sulfide ore typically consist of an anastomosing array of veinlets and stringers in a matrix of crushed and sheared quartz and calcite gangue. The principal ore mineral is argentiferous galena that contains submicroscopic inclusions of freibergite $(\text{Ag,Cu})_{12}(\text{Sb,As})_4 \text{S}_{13}$ (?) and pyrargyrite $(\text{Ag}_3 \text{Sb S}_3)$ (?). Also present in varying amounts are pyrite, hematite, limonite, sphalerite, chalcopyrite, malachite, covellite, cerussite(?), and bornite. Ore minerals were identified by a combination of reflected light microscopy and electron microscopy.

Polished thin sections of wallrock adjacent to mineralized structures and of interstitial gangue minerals in sulfide-bearing veins indicate that sericitic alteration and silicification are closely associated with mineralization. Hand samples of fault breccia commonly contain breccia clasts that are cemented by drusy quartz and stained by malachite and azurite. Although the surface expression of mineralized structures commonly is marked by iron oxide minerals, underground observations

indicate that less mineralization occurred in areas characterized by abundant argillic alteration.

A notable difference between Boulder Basin ores and other tin-bearing deposits in the black shale belt is the reported association of gold with the base-metal assemblage in Boulder Basin. Umpleby (1915) indicated that the original Golden Glow group of claims contained 0.32–0.63 ounces of gold per ton. Hall (1987, p. 134) also reported the presence of gold in the Boulder Basin mineral assemblage. Gold was detected in the present study, but the analytical technique employed is not sensitive to the low concentrations.

Ore Geochemistry

Geochemical studies in the 1970's, later published by Tschanz and Kiilsgaard (1986) suggested that significant tin resources may be present in the black shale belt from Boulder Basin to the Salmon River. Concentrations of tin of as high as 6 weight percent were reported by Tschanz and Kiilsgaard (1986) from base-metal veins that were mined principally for their silver, lead, and zinc content. Hall (1987) stated that T.H. Kiilsgaard, F.S. Fisher, and R.M. O'Leary of the U.S. Geological Survey resampled the vein that Tschanz and Killsgaard had sampled and obtained tin values of approximately one-third the concentrations given by Tschanz and Kiilsgaard (1986). No reason was stated by Hall (1987) for the discrepancy in tin values.

On the basis of discussions with T.H. Kiilsgaard, I believe that the material sampled by Hall (1987) is similar to material sampled by Tschanz and Kiilsgaard (1986). Hall (1987) reported that portions of two of the original samples collected



Figure 7. Photograph of some of the old buildings at the mine town that was built in Boulder Basin. The mill in the left-central part of the photograph, the newest structure at the site, was built in the 1930's when the mine was reopened.

by Tschanz and Kiilsgaard (1986) were resubmitted for analysis and the tin values were significantly lower than those reported in Tschanz and Kiilsgaard (1986). The highest tin values reported in Tschanz and Kiilsgaard (1986) were averages of values determined by chemical, X-ray fluorescence, and atomic absorption techniques (Hall, 1987, p. 134). Hall (1987) used a combination of atomic absorption and semiquantitative emission spectrography to test the new samples. A likely explanation for the discrepancy of tin values between Tschanz and Kiilsgaard (1986) and Hall (1987) is differences in accuracy and precision associated with the different analytical techniques.

As part of the present study, 38 highly mineralized samples were collected from underground mine workings and mine dumps in and adjacent to Boulder Basin. The most highly mineralized samples were selectively collected based on a visual examination. This sampling procedure was implemented to detect tin-bearing minerals within the ore mineral assemblage. The samples were powdered to -200 mesh and analyzed by the U.S. Geological Survey, Denver, Colorado, using a six-step semiquantitative spectrographic analysis. This method has a 10 ppm limit of detection for tin and was considered satisfactory for the objectives in this study. Because the geochemical data are semiquantitative, a rigorous analysis of the data is impossible; however the geochemical data are useful in identifying ore samples that contain anomalous amounts of tin. The results of the analyses (table 1) do not reflect average ore grades.

The highest concentration of tin in the 38 samples is 1,000 ppm. Thirteen of the 38 samples contained at least 100 ppm tin, which is considered to be anomalous on the basis of concentrations in similar ore deposits (Tschanz and Kiilsgaard, 1986; Hall, 1987). Fifteen samples had tin values of 10-50 ppm, and 10 samples had tin concentrations below the limit of detection.

Silver, copper, and antimony (table 1) are plotted versus tin in figure 8. The Ag-Sn plot and the Cu-Sn plot both show a moderately positive correlation, whereas the Sb-Sn plot shows a more scattered distribution. The proportions of silver, copper, antimony, and tin, measured using the electron microprobe (table 2), correlate with the mineral tentatively identified as freibergite(?) ($\text{Ag,Cu}_{12}(\text{Sb,As})_4\text{S}_{13}$). The positive correlation of silver, copper, and antimony with tin may be a result of undetected quantities of stannite ($\text{Cu}_2\text{Fe,Sn,S}_4$) and pyrargyrite ($\text{Ag}_3\text{Sb}_3\text{S}_3$) within the ore mineral assemblage.

Referring to tin-bearing veins in the black shale belt, Hall (1987) stated that "the higher tin values are present where the ores contain high silver and antimony and, at Boulder Basin, high gold values." The present study indicates that silver and copper are more closely correlated with tin than are antimony or gold; however, all samples from this study have gold at or below the detection limit of semiquantitative emission spectrographic analysis (table 1) so no correlations can be calculated.

Ore Microscopy and Electron Microprobe Results

Identification of the different sulfide minerals was done using reflected light microscopy and an electron microprobe. Limited observations suggest that the paragenetic sequence,

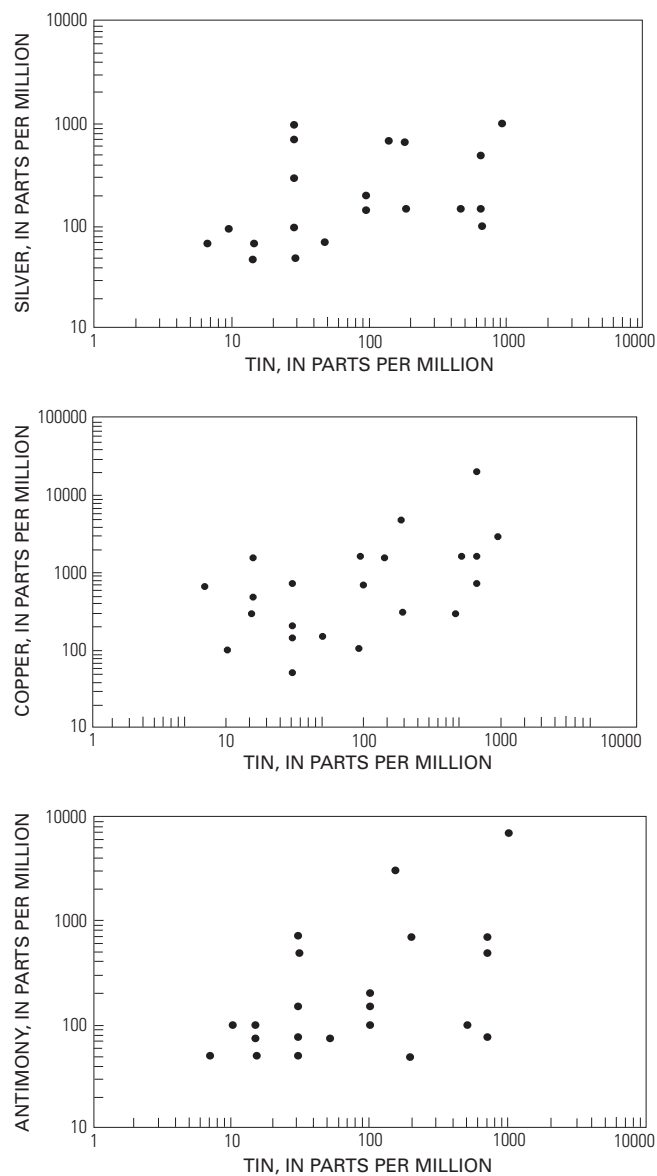


Figure 8. Concentrations of silver, copper, and antimony versus tin in ore samples from Boulder Basin.

from earliest to latest, is sphalerite, chalcopyrite, and galena. Paragenetic relations among pyrite, hematite, limonite, malachite, covellite, cerussite(?), bornite, freibergite(?), and pyrargyrite(?) are not clear.

Several textures were noted in the ore mineral assemblage, and these could be either primary or secondary in origin. Sphalerite rimming both galena and pyrite along grain boundaries was routinely observed. Sphalerite with a patchy sievelike appearance that resembles an exsolution texture also forms in galena (fig. 9). Another light-gray mineral phase along grain boundaries of galena was tentatively identified as cerussite(?). Chalcopyrite locally is altered to deep-blue, fibrous crystals of covellite.

Secondary textures resulting from deformation were routinely encountered. In polyminerallic ores such as these, deformation textures may be evident only in some minerals. For example, pyrite was commonly observed with brittle fractures

Table 1. Geochemical analysis of selected high-grade ore specimens from Boulder Basin, central Idaho.

[Fe, Mg, Ca, and Ti in weight percent; all other elements in parts per million; lower limits of determination shown for each element. G, detected in quantity greater than value shown; L, detected but below the limit of determination; N, not detected. Geochemical analysis by US. Geological Survey, Denver, Colorado, using six step semiquantitative spectrographic methods]

Sample No.	Fe 0.05%	Mg 0.02%	Ca 0.05%	Ti 0.002%	Mn 10 ppm	Ag 0.5 ppm	As 200 ppm	Au 10 ppm	B 10 ppm	Ba 20 ppm	Be 1 ppm	Bi 10 ppm	Cd 20 ppm	Co 5 ppm	Cr 10 ppm	Cu 5 ppm	La 20 ppm
161A	2	L	L	0.01	10	700	L	L	20	N	N	L	50	N	L	1,500	N
161B	0.7	L	N	0.007	L	300	N	N	L	N	N	L	L	N	L	700	N
117	0.5	0.02	L	L	30	500	N	N	L	100	N	L	30	N	L	1,500	N
95	10	0.7	5	0.1	1,000	15	N	N	N	20	L	10	30	7	70	1,500	N
190	2	0.1	0.5	0.05	100	50	N	N	10	30	N	L	20	N	20	1,500	N
448	0.3	L	N	0.005	N	1,000	N	L	20	N	N	10	50	N	L	3,000	50
19	1.5	1.5	2	0.2	700	5	N	N	300	700	L	N	N	7	70	20	N
403	0.2	0.02	N	0.015	15	700	N	N	10	50	N	N	50	N	10	200	N
429	5	L	L	0.02	10	150	200	N	N	L	N	N	N	N	15	700	N
415	15	L	N	0.015	L	200	300	L	N	50	N	N	L	N	15	1,500	N
413	0.5	0.05	0.1	L	70	50	N	N	L	N	N	10	30	N	20	50	N
449	7	0.15	L	0.07	20	150	N	N	N	300	N	L	L	N	20	1,500	N
530	0.7	0.05	N	0.01	20	1	N	N	10	N	N	N	N	N	15	50	N
425	0.7	0.02	L	0.03	20	70	N	N	20	70	N	N	100	N	20	150	N
25	0.2	L	0.05	N	30	15	N	N	L	N	N	N	20	N	20	20	N
452	10	0.02	L	L	200	70	200	N	N	N	L	N	N	7	L	500	N
489A	1	0.02	L	0.01	20	150	L	N	L	N	N	N	L	L	30	300	20
489B	2	0.02	L	0.02	10	15	N	N	10	70	N	N	N	N	15	700	20
487	1.5	L	L	0.02	L	30	L	N	20	700	N	N	N	5	20	150	N
244	5	0.1	N	0.05	50	150	N	N	20	30	N	N	50	N	30	100	70
429A	1	0.02	N	0.02	10	5	N	N	70	50	N	N	N	N	30	30	N
204	0.2	L	0.15	L	70	15	N	N	L	N	N	N	N	N	10	100	N
348	0.3	0.05	0.2	0.01	50	20	N	N	10	50	N	N	20	N	30	20	N
95A	5	L	1.5	0.2	200	1.5	N	N	500	1,000	N	N	L	L	150	70	20
105	1.5	L	0.7	0.2	150	2	N	N	15	500	N	L	L	L	100	150	30
392	0.2	L	N	0.007	L	150	N	N	L	30	N	L	N	N	L	300	70
528	15	0.03	N	L	50	2	N	N	N	N	N	10	N	20	30	200	N
447	0.5	L	N	L	15	100	N	N	10	N	N	N	30	N	10	700	N
454	7	0.2	0.3	0.1	100	50	N	N	10	300	N	N	50	5	50	200	100
429B	1.5	0.02	N	0.02	10	70	L	N	15	70	N	N	L	N	20	300	N
478	7	0.15	L	0.02	30	150	700	N	L	50	N	10	L	N	30	700	N
531	2	0.3	L	0.015	150	70	N	N	L	N	L	N	20	N	20	700	N
426	1	L	N	0.002	20	1,000	300	L	20	50	N	L	L	N	50	150	N
560	1.5	1.5	0.7	0.2	300	30	N	N	200	200	N	N	N	7	150	20	20
161C	7	0.03	L	0.015	30	100	N	N	10	N	N	N	20	20	20	20,000	N
161D	5	1.5	L	0.2	500	50	N	N	L	1,000	N	N	L	30	700	300	50
478A	L	L	L	0.015	10	100	N	N	15	50	N	N	L	N	20	100	N
161E	10	0.05	L	0.02	20	700	L	L	L	100	L	L	20	15	50	5,000	N

Table 1. Geochemical analysis of selected high-grade ore specimens from Boulder Basin, central Idaho—*Continued.*

[Fe, Mg, Ca, and Ti in weight percent; all other elements in parts per million; lower limits of determination shown for each element. G, detected in quantity greater than value shown; L, detected but below the limit of determination; N, not detected. Geochemical analysis by US. Geological Survey, Denver, Colorado, using six step semiquantitative spectrographic methods]

Sample No.	Mo	Nb	Ni	Pb	Sb	Sc	Sn	Sr	V	W	Y	Zn	Zr	Th	Latitude (N)	Longitude (W)
Lower limit	5 ppm	20 ppm	5 ppm	10 ppm	100 ppm	5 ppm	10 ppm	100 ppm	10 ppm	50 ppm	10 ppm	200 ppm	10 ppm	100 ppm		
161A	N	N	L	G20,000	3,000	N	150	N	L	N	15	10,000	70	N	43°50'40"	114°30'24"
161B	N	N	5	G20,000	500	N	30	N	N	N	N	L	50	N	43°50'40"	114°30'24"
117	15	N	L	G20,000	500	N	700	N	L	N	N	10,000	N	N	43°49'55"	114°30'24"
95	5	N	100	500	N	N	N	100	70	N	L	700	50	N	43°48'51"	114°30'39"
190	20	N	30	10,000	N	N	15	L	70	N	N	7,000	50	N	43°49'57"	114°30'13"
448	10	N	L	G20,000	7,000	N	1,000	N	N	N	30	200	50	N	43°50'38"	114°30'29"
19	L	N	50	200	N	7	N	L	50	N	15	N	50	N	43°49'03"	114°30'19"
403	10	N	7	G20,000	700	N	30	L	N	N	N	300	70	N	43°50'54"	114°30'42"
429	5	N	L	10,000	150	N	100	N	L	N	N	200	100	N	43°50'33"	114°30'35"
415	N	N	L	20,000	200	N	100	N	10	N	200	3,000	100	N	43°50'40"	114°30'38"
413	50	N	7	20,000	N	N	30	N	L	N	N	5,000	N	N	43°50'41"	114°30'46"
449	20	N	L	G20,000	100	N	100	100	50	N	N	10,000	70	N	43°50'05"	114°30'47"
530	5	N	10	70	N	N	N	N	L	N	N	500	70	N	43°50'01"	114°30'00"
425	L	N	5	10,000	L	N	50	N	10	N	N	60,000	100	N	43°50'40"	114°30'33"
25	N	N	5	20,000	N	N	N	N	N	N	N	5,000	N	N	43°50'22"	114°29'53"
452	30	N	20	7,000	100	N	15	L	L	N	10	G10,000	N	N	43°50'24"	114°31'03"
489A	200	N	7	1,500	N	N	200	N	L	N	100	200	100	N	43°50'56"	114°30'42"
489B	15	N	5	2,000	L	N	100	N	L	N	N	L	150	N	43°50'56"	114°30'42"
487	L	N	10	1,500	N	N	15	N	L	N	N	N	150	N	43°50'39"	114°30'31"
244	10	N	5	G20,000	100	N	100	N	10	N	10	3,000	100	N	43°51'53"	114°30'54"
429A	L	N	5	150	L	N	N	N	L	N	N	N	150	N	43°50'33"	114°30'35"
204	10	N	L	3,000	L	N	50	N	L	N	N	5,000	N	N	43°50'12"	114°30'36"
348	L	N	5	1,500	L	N	L	N	20	N	N	2,000	N	N	43°50'57"	114°31'00"
95A	L	N	50	70	L	7	N	150	200	N	L	500	50	N	43°48'51"	114°30'39"
105	7	N	30	150	N	5	15	200	50	N	L	500	70	N	43°49'21"	114°30'26"
392	200	N	L	G20,000	100	N	500	200	L	N	N	200	70	N	43°51'19"	114°30'54"
528	L	N	30	70	N	N	N	N	10	N	10	300	N	N	43°48'45"	114°30'02"
447	L	N	L	20,000	150	N	30	N	L	N	N	500	N	N	43°50'35"	114°30'32"
454	15	N	100	7,000	L	L	30	N	100	N	30	G10,000	30	N	43°50'31"	114°30'52"
429B	7	N	L	1,500	L	N	15	N	L	N	N	700	100	N	43°50'33"	114°30'35"
478	15	N	5	20,000	700	N	700	N	10	N	20	500	100	N	43°50'38"	114°30'35"
531	15	N	7	1,000	N	N	N	N	10	N	N	G10,000	50	N	43°50'06"	114°30'02"
426	L	N	5	G20,000	700	N	30	N	N	N	30	N	10	N	43°50'38"	114°30'33"
560	L	N	50	1,000	N	10	N	L	70	N	L	N	50	N	43°50'19"	114°31'19"
161C	15	N	100	2,000	L	N	700	N	15	N	30	G10,000	100	N	43°50'40"	114°30'24"
161D	L	N	2,000	7,000	N	15	15	700	70	N	10	L	70	N	43°50'40"	114°30'24"
478A	L	N	L	2,000	100	N	10	N	L	N	50	200	150	N	43°50'38"	114°30'35"
161E	5	N	70	G20,000	700	N	200	N	15	N	15	200	200	N	43°50'40"	114°30'24"

Table 2. Microprobe analyses of galena from Boulder Basin, central Idaho, Idaho, in weight percent.

Sample No.	As	Zn	Cu	Fe	S	Pb	Ag	Mn	Sb	Sn	Total wt. percent	Latitude (N)	Longitude (W)
161C, point C	0.00	0.02	0.04	0.01	13.19	86.21	0.04	0.00	0.06	0.03	99.61	43°50'40"	114°30'24"
161C, point G	0.00	0.02	0.00	0.01	13.15	86.61	0.02	0.00	0.16	0.04	100.01	43°50'40"	114°30'24"
161D, point A	0.00	0.00	0.03	0.00	13.02	85.97	0.12	0.00	0.17	0.07	99.38	43°50'40"	114°30'24"
161D, point B	0.00	0.00	0.00	0.01	13.36	86.22	0.00	0.04	0.08	0.08	99.79	43°50'40"	114°30'24"
161D, point C	0.18	0.01	0.00	0.00	13.20	86.19	0.08	0.01	0.11	0.00	99.78	43°50'40"	114°30'24"
117, point A	0.00	0.01	0.03	0.03	13.48	86.20	0.00	0.07	0.03	0.06	99.90	43°49'55"	114°30'24"
117, point A-1	0.00	0.00	0.00	0.04	13.45	86.40	0.03	0.00	0.01	0.00	99.93	43°49'55"	114°30'24"
117, point B	0.00	0.00	0.01	0.00	13.43	85.60	0.04	0.00	0.00	0.00	99.09	43°49'55"	114°30'24"
117, point D	0.00	0.00	0.03	0.00	13.31	86.32	0.02	0.02	0.00	0.02	99.72	43°49'55"	114°30'24"
117A, point A	0.29	0.00	0.01	0.01	12.95	85.85	0.10	0.00	0.14	0.00	99.35	43°49'55"	114°30'24"
348, point A	0.00	0.00	0.00	0.00	13.11	86.63	0.13	0.02	0.24	0.00	100.12	43°50'57"	114°31'00"
392, point B	0.18	0.00	0.00	0.00	13.29	87.25	0.03	0.00	0.00	0.00	100.76	43°51'19"	114°30'54"
392, point B-1	0.00	0.09	0.00	0.00	13.28	86.55	0.00	0.05	0.03	0.00	100.00	43°51'19"	114°30'54"
392, point B-2	0.00	0.00	0.02	0.00	13.48	85.90	0.00	0.01	0.02	0.00	99.44	43°51'19"	114°30'54"
448, point A-1	0.00	0.00	0.00	0.04	12.97	85.43	0.17	0.01	0.08	0.00	98.69	43°50'38"	114°30'29"
448, point A-2	0.00	0.03	0.01	0.01	13.30	85.75	0.38	0.05	0.50	0.02	100.02	43°50'38"	114°30'29"
448, point B	0.14	0.02	0.00	0.04	12.80	85.25	0.24	0.03	0.11	0.00	98.60	43°50'38"	114°30'29"
448, point C	0.00	0.00	0.00	0.00	13.50	87.65	0.09	0.06	0.11	0.00	101.41	43°50'38"	114°30'29"
448, point C-1	0.00	0.00	0.00	0.03	13.36	85.78	0.12	0.07	0.16	0.00	99.51	43°50'38"	114°30'29"
116C, point F*	0.00	5.42	15.67	3.72	21.66	1.07	27.16	0.00	24.80	0.15	99.63	43°50'40"	114°30'24"
448, point B-1**	0.02	0.00	0.86	0.00	13.20	67.90	18.67	0.00	2.78	0.00	103.43	43°50'40"	114°30'29"

* Freibergite(?)

** Galena with microinclusion of pyargyrite(?)

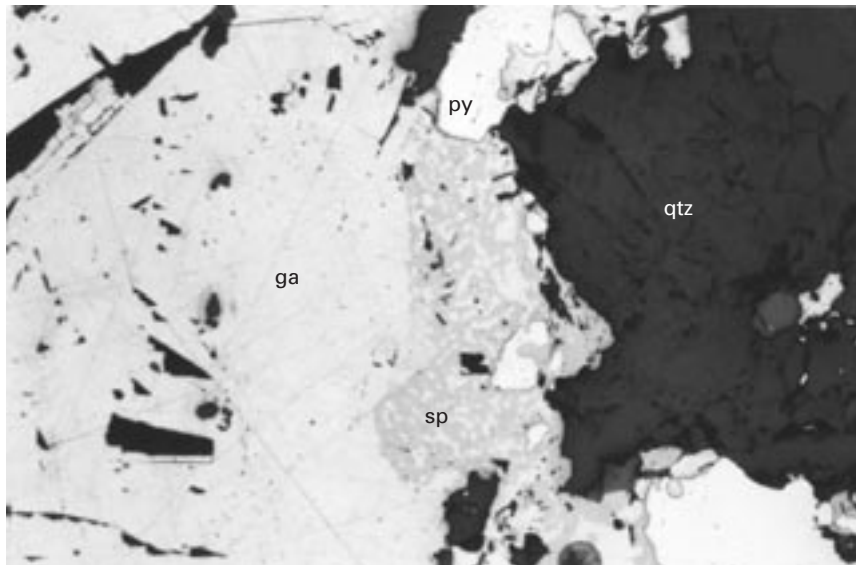


Figure 9. Photomicrograph of mineralized sample from Boulder Basin. Light-gray sphalerite (sp) imparts a distinctive sievelike texture in galena (ga). Quartzite (qtz) wallrock is dark-gray, and pyrite (py) is white. Field of view 2.0 mm.

that are filled with softer minerals such as galena and sphalerite. However, most of the deformation in the ore mineral assemblage is reflected in galena, the softest sulfide present in these ores. Triangular cleavage pits are diagnostic features for the identification of galena, and according to Craig and Vaughan (1981) they are a measure of deformation. Flattened and contorted triangular cleavage pits in galena were commonly noted in optical examination and their presence suggests that the ores were deposited prior to, or synchronously with, deformation.

Some of the chemical analyses from the microprobe examination are given in table 2. Two of the samples analyzed appeared optically to be galena, however, the atomic ratios are not indicative of that mineral. This discrepancy is thought to be a result of submicroscopic inclusions of freibergite(?) and pyrargyrite(?), on the basis of comparison of chemical formulas for those minerals with the atomic ratios from the microprobe analyses. Although sample 116C lacks detectable arsenic (table 2), otherwise the chemical analysis for this sample approximates that of the mineral freibergite ($(\text{Ag,Cu})_{12}(\text{Sb,As})_4\text{S}_{13}$, which is isomorphous with tetrahedrite ($(\text{Cu,Fe})_{12}\text{Sb}_4\text{S}_{13}$). The chemical analysis for sample 448 B-1 is thought to indicate a mixture of galena and pyrargyrite and the result of the electron beam intersecting the grain boundaries between the two minerals. Dark-red sulfide inclusions within galena crystals were noted in the hand specimen used to make the thin section for point 448 B-1 (table 2). Pyrargyrite is commonly referred to as “ruby silver” in the literature and it forms small red inclusions within galena and other sulfides according to Dana (1977, p. 257).

Hall and Czamanske (1972) also reported five distinct microinclusions in galena, including freibergite, from the Wood River area. They indicated that the inclusions are normally on the order of two or three microns in size and are difficult to observe optically because of the high reflectance of galena. Most of the silver in Boulder Basin ores likely is in the submicroscopic inclusions in galena.

No discrete tin-bearing phases were detected in this study. The paucity of tin-bearing minerals such as stannite may be attributed to one or more of the following reasons:

1. Tin-bearing minerals were present in portions of a sample analyzed geochemically but not in the portion of the sample used to make thin sections.

2. Submicroscopic tin-bearing minerals may have been present in the polished thin sections, but because of their extremely small size they may have been overlooked during the optical examination. Also if such microinclusions were present, they were not in the particular parts of the thin sections that were analyzed using the electron microprobe.

3. Tin-bearing minerals are not present in the samples that were collected in this study. Anomalous concentrations of tin from the geochemical analyses are attributed solely to solid-state solution of tin within the lattices of freibergite, galena, and sphalerite.

Because Hall (1987) reported the presence of minor to trace concentrations of stannite and cassiterite in Boulder Basin ores, the second hypothesis likely explains the absence of identifiable tin-bearing phases in this study.

Geophysical Signature

Preliminary airborne magnetic data compiled during the U.S. Geological Survey Conterminous United States Mineral Assessment Program (CUSMAP) of the Hailey $1^\circ \times 2^\circ$ quadrangle suggest that a large intrusion is present beneath Boulder Basin (M.D. Kleinkopf, written commun., 1995). This observation is consistent with the large volume of Tertiary hypabyssal rocks mapped in the Paleozoic strata in Boulder Basin (fig. 6).

As part of the Hailey CUSMAP study, color contoured maps were generated from aeroradiometric data collected by

National Uranium Resource Evaluation (NURE) The original airborne NURE data were manipulated to produce maps showing high concentrations of the radioactive element suite potassium-uranium-thorium in the Boulder Basin area. The source of the potassium, uranium, and thorium is interpreted to be the highly evolved pink granite and rhyolite porphyry, both of which contain anomalous concentrations of radiogenic elements (Bennett and Knowles, 1985, p. 87). There is a good correlation between the positive magnetic anomalies, associated with exposures of pink granite and rhyolite porphyry, and the anomalous concentrations of radiogenic elements in the NURE data in Boulder Basin (M.D. Kleinkopf, written commun., 1995). Because the ore deposits in Boulder Basin are spatially associated with rhyolite porphyry, geophysical and radiogenic methods may be useful tools to identify additional areas of mineralization.

Genesis and Ore Controls

The Tertiary hypabyssal complex that intruded the Milligen and Wood River Formations in Boulder Basin was the likely heat source for the hydrothermal system responsible for ore deposits. The fact that andesite, dacite and rhyolite porphyries are propylitically altered throughout the study area is consistent with the hypothesis that the intrusions were altered by hydrothermal fluids that were produced during magmatic emplacement. No intrusive rocks younger than Eocene in age have been reported in the Boulder Basin area.

A convective hydrothermal cell of circulating solutions that propagated through fractured strata and eventually precipitated metals within structurally high level Tertiary faults is postulated in Boulder Basin. Hydrothermal solutions leached base metals from the carbonaceous rocks in the Milligen Formation. Tin and gold were possibly introduced into the hydrothermal system from Tertiary intrusions, such as the intrusions that formed the highly evolved pink granite. Tertiary granite in central Idaho contains, on average, two or three times more uranium, thorium, and ^{40}K than do rocks of the Cretaceous Idaho batholith; it also has a high content of large cation elements, including tin (Bennett and Knowles, 1985).

Mineralized rock is commonly present where Tertiary faults cut sedimentary strata and is virtually absent where the faults cut intrusive rocks. This suggests that the chemistry of the host rock was a controlling factor for ore deposition. If the ore solutions were acidic, then CO_3 in the sedimentary strata could have buffered the solution, resulting in deposition of the sulfides.

The rheological character of the sedimentary strata may have also been a factor for ore deposition. Highly competent massive quartzite of the Wood River Formation is more amenable to structural openings during brittle faulting than are the less competent shale of the Milligen Formation. The ore-forming solutions could precipitate in a highly fractured brittle host rock. The fact that the main mine workings at Boulder Basin are hosted by calcareous, massive quartzite of the Wood River Formation supports this assertion. Both stratigraphic and structural controls, in conjunction with widespread plutonism, resulted in a favorable geologic environment for development of Boulder Basin ores.

Potential for Economic Tin Mineralization

The geologic setting, host rock, source rock, and age of mineralization in Boulder Basin are similar to those of known tin-bearing base metal ore deposits in the black shale belt of central Idaho, described by Tschanz and Kiilsgaard (1986). The criteria for assessing the potential for economic tin mineralization in Boulder Basin are based on the following parameters:

1. Anomalous concentrations of tin were detected in this study (tables 1, 2).

2. The general type, extent, and size of ore deposits that were observed during field mapping and the examination of underground mine workings.

3. The presence of trace to minor amounts of cassiterite and stannite in Boulder Basin ores (Hall, 1987).

On the basis of the defined parameters, I conclude that it is unlikely that tin will be extracted as a primary commodity from Boulder Basin. The ore deposits are discontinuous low tonnage veins that occur with marginally anomalous concentrations of tin. Hall (1987) reached the same conclusion for tin-bearing base-metal deposits in the black shale mineral belt. The ore deposits in Boulder Basin contain silver, lead, zinc, and gold and tin should be evaluated as a potential byproduct in any future mining operations. Future exploration for tin deposits in the black shale terrane might indicate higher grade or larger tonnage of tin ore within buried shallow-level intrusions similar to known tin porphyries below tin-bearing veins in the Bolivian tin district of South America (Sillitoe and others, 1975; Guilbert and Park, 1986, p. 433–436).

Exploration Guides

Three important characteristics of Bolivian tin deposits (Taylor, 1979) are present in the tin-bearing veins of the black shale belt of central Idaho. (1) Tin and silver are spatially associated with Tertiary high-level subvolcanic intrusions. (2) Thick marine sequences, predominantly shale and sandstone of Paleozoic age, serve as host rocks for many of the tin deposits. (3) Complex polymetallic sulfur-rich ores, including silver sulfosalts and stannite, are present in late-stage veins in most of the tin deposits. The fact that all three of these characteristics are also present in tin-bearing veins of the black shale belt in Boulder Basin suggests that a Bolivian tin deposit model might be useful in the identification of similar deposits in south-central Idaho.

Ore deposits in Boulder Basin are probably confined to areas that contain carbonaceous source rocks with naturally occurring, high concentrations of base metals. Competent, calcareous, siliclastic strata that have been fractured would serve as host rocks for chemically reactive ore solutions. Tertiary normal faults and widespread emplacement of highly evolved Tertiary intrusions are also good indicators of ore deposits. Silicification and sericitic alteration associated with Bolivian tin deposits should be identified and correlated with Tertiary structures in Boulder Basin. Pathfinder elements such as antimony, tin, arsenic, mercury, and silver probably correlate with gold- and

tin-bearing base-metal veins throughout the black shale terrane (Tschanz and Kiilsgaard, 1986, p. 90; Smith, 1995) and may help identify buried deposits.

Once areas of potential mineralization are delineated, detailed geophysical ground surveys utilizing magnetic and electromagnetic very low frequency (VLF) techniques are very effective tools for locating ore deposits. Together the two techniques provide a good resolution for locating planar faults that contain conductive base metals.

Observations made during this study indicate that the areas that most completely reflect the described characteristics of Bolivian tin deposits are south from Boulder Basin to the North Fork of the Big Wood River, north of the Boulder Basin to the Salmon River, and west of the Boulder Basin within the Smoky Mountains.

References

- Armstrong, R.E., 1975, The geochronometry of Idaho: Isochron West, no.14, p. 1–50.
- Bennett, E.H., and Knowles, C.R., 1985, Tertiary plutons and related rocks in central Idaho, *in* McIntyre, D.H., ed., Symposium on the geology and mineral deposits of the Challis 1°×2° quadrangle, Idaho: U.S. Geological Survey Bulletin 1658, p. 81–95.
- Craig, J.R., and Vaughan, D.J., 1981, Ore microscopy and ore petrography: New York, John Wiley and Sons, 406 p.
- Dana, J.D., 1977, Manual of mineralogy (19th ed.): New York, John Wiley and Sons, 532 p.
- Guilbert, J.M., and Park, C.F. 1986, The geology of ore deposits: W.H. Freeman and Company, 985 p.
- Hall, W.E., 1985, Stratigraphy of and mineral deposits in middle and upper Paleozoic rocks of the black-shale mineral belt, central, Idaho, *in* McIntyre, D.H., ed., Symposium on the geology and mineral deposits of the Challis 1°×2° quadrangle, Idaho: U.S. Geological Survey Bulletin 1658, p. 117–131.
- Hall, W.E., 1987, Lead-silver-zinc-antimony-tin vein deposits, *in* Fisher, F.S., and Johnson, K.M., eds., Preliminary manuscript for mineral-resource potential and geology of the Challis 1°×2° quadrangle, Idaho: U.S. Geological Survey Open-File Report 87-480, p.133–140.
- Hall, W.E., Batchelder, J., and Douglass, R.C., 1974, Stratigraphic section of the Wood River Formation, Blaine County, Idaho: U.S. Geological Survey Journal of Research, v. 2, no. 1, p. 89–95.
- Hall, W.E., and Czamanske, G.K., 1972, Mineralogy and trace element content of the Wood River lead-silver deposits, Blaine County, Idaho: Economic Geology, v. 67, no. 3, p. 350–361.
- Hall, W.E., Rye, R.O., and Doe, B.R., 1978, Wood River mining district, Idaho: Intrusion related lead-silver deposits derived from country rock source: U.S. Geological Survey Journal of Research, v. 6, no. 5, p. 579–592.
- Johnson, K.M., Lewis, R.S., Bennett, E.H., and Kiilsgaard, T.H., 1988, Cretaceous and Tertiary intrusive rocks of south-central Idaho, *in* Link, P.K. and Hackett, W.R., eds., Guidebook to the geology of central and southern Idaho: Idaho Geological Survey Bulletin 27, p. 55–86.
- Paul, E.K., Jr., 1981, Tin deposits of the Galena district, Blaine County, Idaho: Moscow, University of Idaho, M.S. thesis, 112 p.
- Ramsay, J.G., and Huber, M.I., 1983, Strain analysis: London, Academic Press, 307 p.
- Ratchford, M.E., 1989, Geology of the Boulder Basin, Blaine and Custer Counties, Idaho: Moscow, University of Idaho, M.S. thesis, 153 p.
- Ratchford, M.E., and Reid, R.R., 1993, Structural analysis of compressional and extensional deformation within the Wood River and Milligen Formations, south-central, Idaho: Geological Society of America Abstracts with Programs, v. 25, no. 5, p. 137.
- Sandberg, C.A., Hall, W.E., Batchelder, J.N., and Axelsen, C., 1975, Stratigraphy, conodont dating, and paleotectonic interpretation of the type Milligen Formation (Devonian), Wood River Area, Idaho: U.S. Geological Survey Journal of Research, v. 3, no. 6, p. 707–720.
- Sillitoe, R.H., Halls, C., and Grant, J.N., 1975, Porphyry tin deposits: Bolivia: Economic Geology, v. 70, p. 913–927.
- Simpson, C., 1986, Determination of movement sense in mylonites: Journal of Geological Education, v. 34, p. 246–261.
- Smith, C.L., 1995, Interpretation of the regional geochemistry of the Hailey 1°×2° quadrangle, south-central Idaho: U.S. Geological Survey Bulletin 2064-L, 22 p.
- Taylor, R.G., 1979, Geology of tin deposits: Amsterdam, Elsevier, 543 p.
- Tschanz, C.M., and Kiilsgaard, T.H., 1986, Geologic appraisal of the eastern part of the Sawtooth National Recreation Area, Idaho: U.S. Geological Survey Bulletin 1545-C, p. 53–208.
- Turner, R.J.W., and Otto, B.R., 1988, Stratigraphy and structure of the Milligen Formation, Sun Valley area, Idaho, *in* Link, P.K., and Hackett, W.P., eds., Guidebook to the geology of central and southern Idaho: Idaho Geological Survey Bulletin 27, p. 153–167.
- Umpleby, J.B., 1915, Ore deposits in the Sawtooth quadrangle, Blaine and Custer Counties, Idaho, U.S. Geological Survey Bulletin 580, p. 221–249.
- Van Noy, R.M., Ridenour, James, Zilka, N.T., Federspiel, F.E., Evans, R.K., Tuckey, E.T., and McMahan, A.B., 1986, Economic appraisal of the eastern part of the Sawtooth National Recreation Area, Idaho: U.S. Geological Survey Bulletin 1545-E, p. 231–472.
- Worl, R.G., Kiilsgaard, T.H., Bennett, E.H., Link, P.K., Lewis, R.S., Mitchell, V.E., Johnson, K.M., and Snyder, L.D., 1991, Geologic map of the Hailey 1°×2° quadrangle, Idaho: U.S. Geological Survey Open-File Report 91-340, scale 1:250,000.